



The Controlling Factors of the Natural Gas Hydrate Accumulation in the Songnan Low Uplift, Qiongdongnan Basin, China

Yang Wei^{1,2,3,4}, Kuang Zenggui^{3,4}, Ren Jinfeng^{3,4*}, Liang Jinqiang^{3,4}, Lu Hong², Ning Zijie^{3,4}, Xu Chenlu^{3,4}, Lai Hongfei^{3,4}, Chen Rui⁴, Zhao Bin⁴, Chen Jing^{3,4}, Zhang Xi^{3,4} and Liu Lei⁵

¹Southern Marine Science and Engineering Guangdong Laboratory (Guangzhou), Guangzhou, China, ²State Key Laboratory of Organic Geochemistry, Guangzhou Institute of Geochemistry, Chinese Academy of Sciences, Guangzhou, China, ³National Engineering Research Center of Gas Hydrate Exploration and Development, Guangzhou, China, ⁴Guangzhou Marine Geology Survey, China Geological Survey, Guangzhou, China, ⁵Beijing International Engineering Consulting Co., Ltd., Beijing, China

OPEN ACCESS

Edited by:

Lihua Zuo,
Texas A&M University Kingsville,
United States

Reviewed by:

Taohua He,
China University of Petroleum,
Huadong, China
Qilin Xiao,
Yangtze University, China
Wei Zhou,
Southern Marine Science and
Engineering Guangdong Laboratory
(Zhuhai), China

*Correspondence:

Ren Jinfeng
jf_ren@163.com

Specialty section:

This article was submitted to
Marine Geoscience,
a section of the journal
Frontiers in Earth Science

Received: 23 February 2022

Accepted: 11 April 2022

Published: 26 May 2022

Citation:

Wei Y, Zenggui K, Jinfeng R,
Jinqiang L, Hong L, Zijie N, Chenlu X,
Hongfei L, Rui C, Bin Z, Jing C, Xi Z and
Lei L (2022) The Controlling Factors of
the Natural Gas Hydrate Accumulation
in the Songnan Low Uplift,
Qiongdongnan Basin, China.
Front. Earth Sci. 10:882080.
doi: 10.3389/feart.2022.882080

Hydrocarbon charging stages and natural gas hydrate accumulation models were established in the Songnan Low Uplift, Qiongdongnan Basin (QDNB), China. Detailed geochemical analysis, paleotemperature and paleopressure analyses, seismic interpretation, and hydrocarbon charging characterization were conducted to investigate the controlling factors of natural gas hydrate accumulation. The Yacheng and Lingshui formations in the Lingshui Sag were identified as effective source rocks. The $\delta^{13}\text{C}_1$ values of the gas hydrates vary from -35.97% to -59.50% , following a direction from the Sag Center to the Low Uplift, indicating that $\delta^{13}\text{C}_1$ values became relatively lighter during gas migration. Seismic data evidence revealed that large-scale faults, laterally distributed sandstones, and gas chimneys were comprehensive, however efficient hydrocarbon migration pathways. Systematic overpressure was developed in the Yacheng and Huangliu formations, which offer sufficient hydrocarbon migration impetus. Hydrocarbon-bearing aqueous inclusions and their coexisting aqueous inclusions were observed in the Huangliu Formation in the Lingshui Sag, indicating four stages of hydrocarbon charging in the QDNB. Based on the comprehensive analysis in this research, two gas hydrate accumulation models were proposed in the Songnan Low Uplift, QDNB, as follows: 1) a mixture of gas migrated by large-scale faults and a thermogenic-biogenic mixed gas model and 2) gas hydrates from laterally distributed sandstones sealed by MTDs.

Keywords: migration pathway, paleopressure characteristics, hydrocarbon charging stages, gas hydrate accumulation, the Songnan Low Uplift

INTRODUCTION

The Qiongdongnan Basin (QDNB) is located in the northwestern continental margin of the South China Sea, which is a petroliferous Cenozoic basin with strong overpressure being widely developed (Huang et al., 2003; Hao et al., 2007; Zhu et al., 2009; Huang et al., 2012; Huang et al., 2016). A series of large gas fields, including LS25-1, LS17-2, LS18-1, and YL8 gas fields, were discovered in the Neogene Huangliu and Yinggehai formations in the west of the QDNB in the last few decades, with

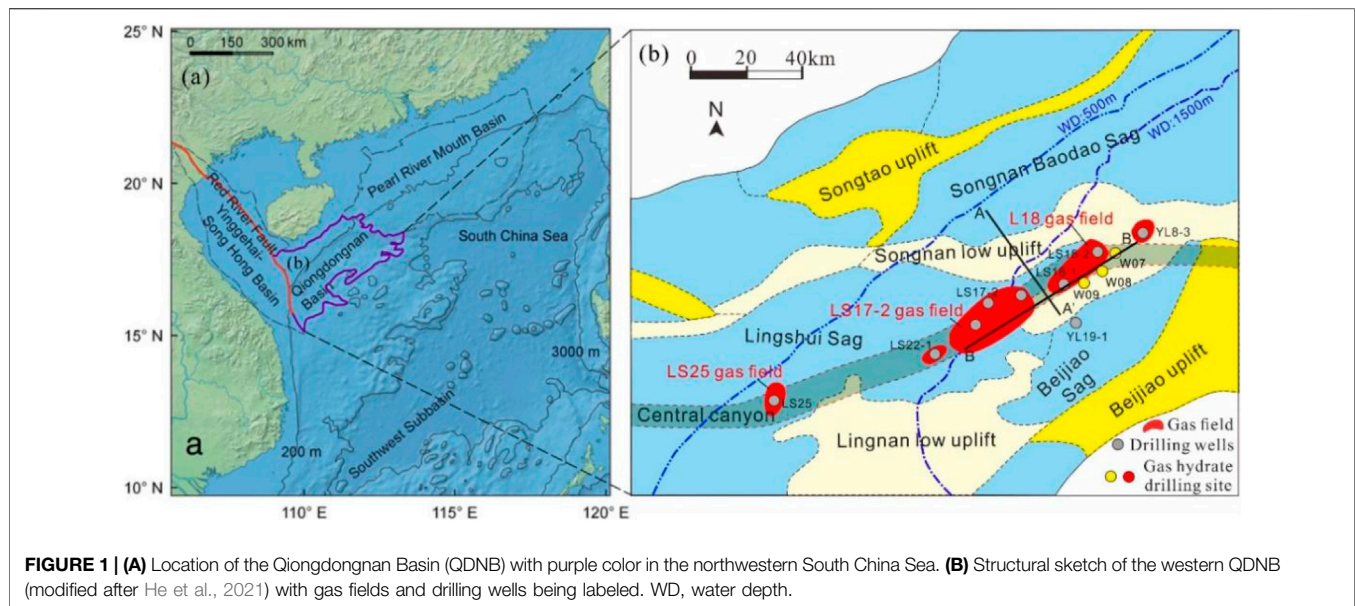


FIGURE 1 | (A) Location of the Qiongdongnan Basin (QDNB) with purple color in the northwestern South China Sea. **(B)** Structural sketch of the western QDNB (modified after He et al., 2021) with gas fields and drilling wells being labeled. WD, water depth.

the main source rocks of the Paleogene Yacheng and Lingshui formations being deposited in a coastal plain or littoral to a neritic environment (Huang et al., 2012; Zhang et al., 2014; Huang et al., 2016; Su et al., 2017; Zhu et al., 2018; Xie et al., 2019; Zhang et al., 2019a, Zhang et al., 2019b, Zhang et al., 2019c; Su et al., 2021). The Yacheng and Lingshui formations of the LS25-1 and LS17-2 gas fields in the Lingshui Sag were overpressured, while the main gas-bearing layers, the Mesozoic granite Yacheng reservoirs of the YL8-1 and YL8-3 gas fields in the Songnan Low Uplift, were normal pressured (Wang et al., 2016; Gan et al., 2019; Shi et al., 2019; Yang et al., 2021).

A clean and efficient energy resource natural gas hydrate has been widely discovered in the QDNB (Zhang et al., 2018; Fang et al., 2019; Liang et al., 2019; Wei et al., 2019; Ye et al., 2019), showing significant exploration potentials in this area. In addition, a number of typical and representative gas hydrates were discovered and are being sampled at sites GMGS5, W07, W08, and W09 by the Guangzhou Marine Geological Survey (GMGS) in 2018, which were identified as typical gas hydrate sites in the Songnan Low Uplift. Stable carbon isotope analysis of the hydrated gas indicated a mixed microbial and thermogenic origin for their formation (Liang et al., 2019; Wei et al., 2019; Ye et al., 2019; Zhang et al., 2020; Lai et al., 2021).

Numerous research studies on the geological, geochemical, and geophysical characteristics of the gas hydrate system have been conducted in the QDNB (Zhang et al., 2018; Liang et al., 2019; Wei et al., 2019; Ye et al., 2019; Deng et al., 2021); however, natural gas hydrate accumulation mechanisms, reservoir characterization, and production trials need further research, especially on the influences of hydrocarbon charge on natural gas hydrate accumulation. The Yacheng and Lingshui formations are the most important source rocks in the Lingshui Sag, which have entered the dry gas window. The overpressured source rock intervals and preferential migration pathways offer continuous gas sources into the hydrate-bearing

reservoirs. As a result, source rock maturations, migration pathways, overpressure, and hydrate-bearing reservoir characteristics co-contribute to natural gas hydrate accumulation.

Aims of this research are to

- (1) investigate the migration pathways and overpressure characteristics of natural gas hydrates in the QDNB;
- (2) clarify the influence of hydrocarbon charge on gas hydrate accumulation;
- (3) understand origins of gas forming the gas hydrates; and
- (4) establish natural gas hydrate accumulation models.

GEOLOGICAL SETTING

The Lingshui Sag is located in the west of the deep-water area of the QDNB (Figure 1). The LS25 gas field is located in the west of the Lingshui Sag, adjacent to the Ledong Sag, and the LS17-2 and LS18 gas fields are located in the eastern slope of the Lingshui Sag (Figure 1B, Yao et al., 2015; Zhang et al., 2016; Huang et al., 2017; Li et al., 2017; Zhang et al., 2019c). Tectonic evolution of the QDNB comprises two stages: rifting from Eocene to Oligocene and a depression stage from Miocene to Quaternary (Hu et al., 2013). The QDNB experienced multi-stage tectonic movements, including Shenhu, Zhujiang, Nanhai, and Dongsha tectonic movements (Wang et al., 2021). Tectonic evolution of the Lingshui Sag is consistent with that of the QDNB, leading to the deposition of 6,000–12,000 m Cenozoic strata (Figure 2), which are divided into eight formations, including the Oligocene Yacheng and Lingshui formations (36–30 Ma and 30–21 Ma), the Miocene Sanya, Meishan, and Huangliu formations (21–15.5 Ma, 15.5–10.5 Ma, and 10.5–5.5 Ma), and the Pliocene Yinggehai Formation (5.5–1.9 Ma) (Figure 2) (Su et al., 2018).

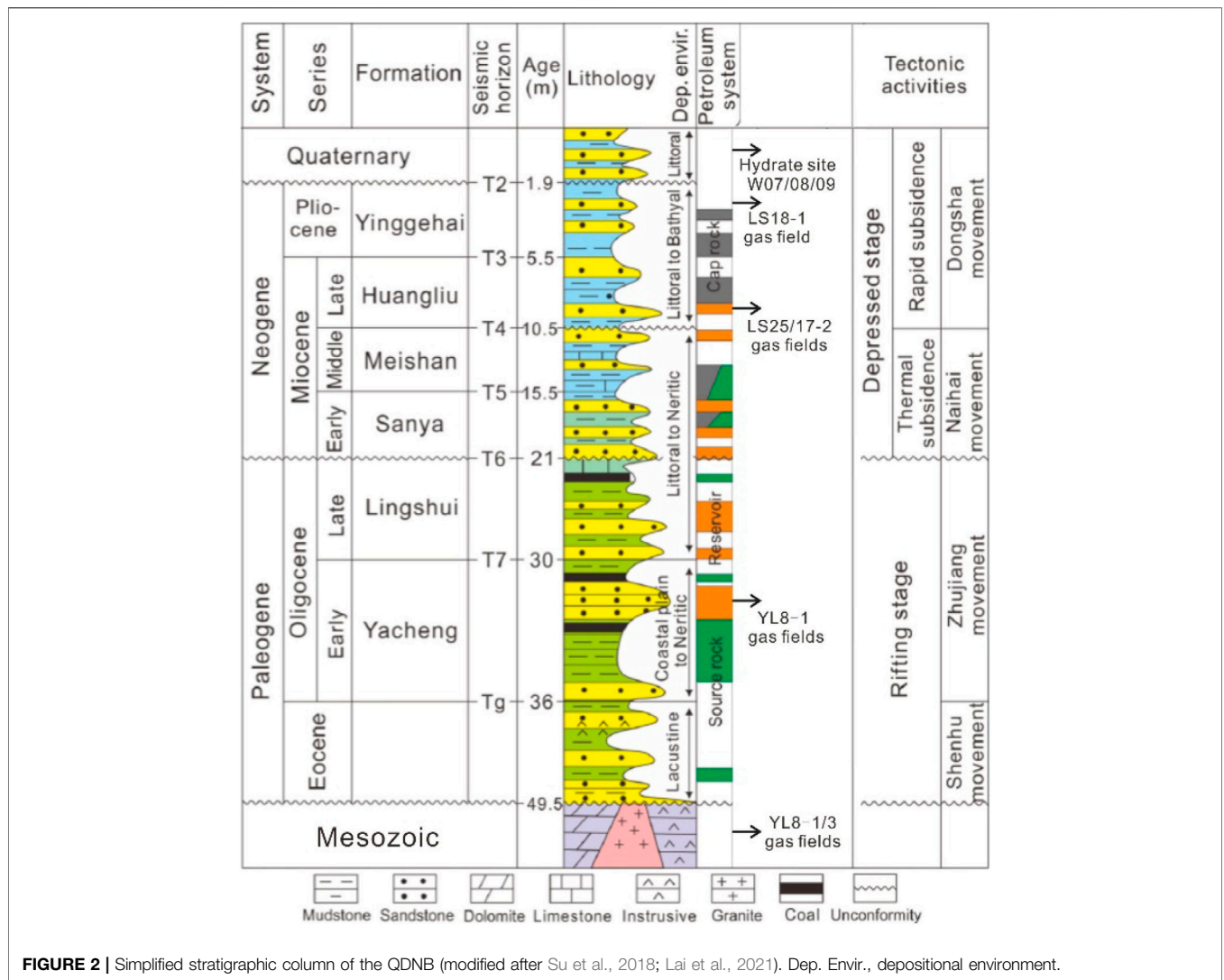


FIGURE 2 | Simplified stratigraphic column of the QDNB (modified after Su et al., 2018; Lai et al., 2021). Dep. Envir., depositional environment.

The Songnan Low Uplift—which is bounded by the Lingshui Sag, the Songnan-Baodao sags, the Changchang Sag, and the Beijiao Sag (**Figure 1B**)—comprises the main targeted areas for natural gas hydrate exploration. Discoveries of the YL8 and YL1 gas fields indicated that the Songnan Low Uplift is an area of natural gas accumulation (Shi et al., 2019; Zhang et al., 2019; Yang et al., 2021), which is also subject to gas hydrate accumulation. Gas-bearing formations of the YL8-1/3, LS25/17-2, and LS18-1 gas fields are mainly the Huangliu, Yinggehai, and Yacheng formations, and the hydrate-bearing formation in the GMGS5-W07/W08/W09 sites are mainly in the Quaternary formation (**Figure 2**).

RESULTS AND DISCUSSION

Gas Source

TOC contents and Rock-Eval parameters were effective to characterize hydrocarbon generation potentials of source rocks

(He et al., 2018; He et al., 2022). TOC contents of the analyzed mudstones, carbonaceous mudstones, and coal samples in the Yacheng and Lingshui formations range from 0.13 wt.% to 96.51 wt.% (**Figure 3A**). Rock-Eval data reveal hydrocarbon generation potentials of free hydrocarbon (S_1) and generative hydrocarbon potential (S_2) of the analyzed samples ranging from 0.02 mg HC/g TOC to 154.05 mg HC/g TOC (**Figure 3A**), which are identified as the main source rocks forming the discovered gas fields. Most of the analyzed samples were characterized as fair to very good source rocks, with carbonaceous mudstones and coal samples being identified as excellent source rocks, indicating great hydrocarbon generation potential for the source rock formations (**Figure 3A**).

Maximum temperature (T_{max}) and hydrogen index (I_H) values show close-set distribution, with T_{max} values ranging from 408 to 482°C and I_H values ranging from 11 mg HC/g TOC to 462 mg HC/g TOC, respectively (**Figure 3B**). The average T_{max} reaches 444°C, and the average I_H value is 101 mg HC/g TOC, indicating

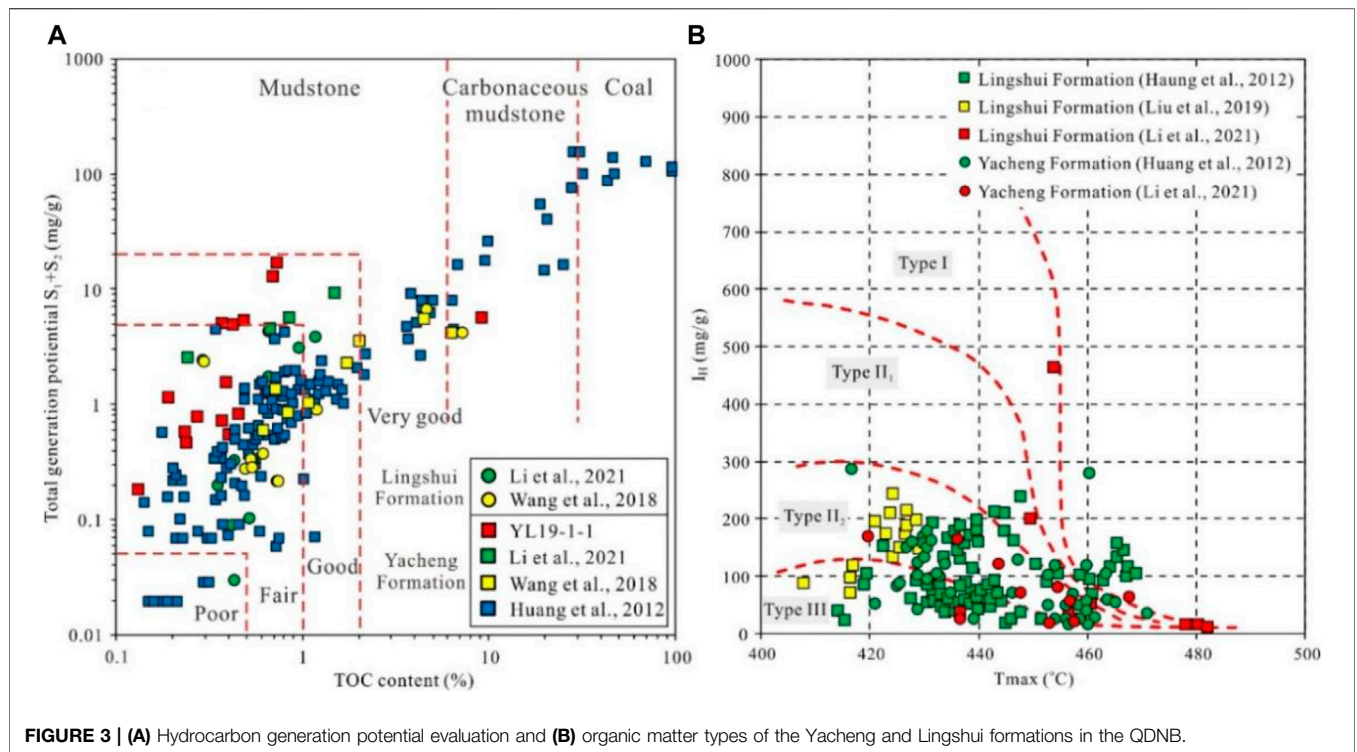


TABLE 1 | Thermal maturity of source rocks, namely, Meishan, Lingshui, and Yacheng formations, in the Sag Center and Low Uplift in the QDNB.

Area	Well	Formation	T _{max} (°C)	R _o (%)	Data source
Sag Center	L25-2	Yacheng	/	>2.0	Zhang et al. (2019c)
	L25-1	Meishan	/	0.80	
Low Uplift	LS33-1	Lingshui	/	0.79	Wang et al. (2018)
	YL19	Lingshui	422	0.51	
	LS33	Lingshui	424	0.49	He, (2020)
	YL19	Yacheng	474	1.14	
	YL8	Yacheng	/	1.52–1.70	Li et al. (2020)

that source rocks of the Yacheng and Lingshui formations are sufficiently mature to generate dry gas. In the T_{max} versus I_H plots (Figure 3B), most of the analyzed samples were considered to be Type II₂ and III kerogens, with a smaller number of analyzed samples being characterized as Type II₁ kerogen (Figure 3B).

Vitrinite reflectance (R_o%) was measured to assess thermal maturities of the source rocks in this research. R_o% values of the samples in the Yacheng Formation are >2.0% in the Lingshui Sag, a higher value than that of the samples in the Low Uplift (Table 1). The results indicate that the Yacheng and Lingshui formations in the QDNB are highly matured to over-matured.

Natural gas compositions in the LS25, LS17-2, LS18-1, YL8-1, and YL8-3 gas fields and the GMGS5-W08 hydrate site are dominated by hydrocarbon gas, accounting for 76.38–99.79% of the total gas volumes (Table 2). Methane (CH₄) contents of the gas fields and the GMGS5-W08 gas hydrate site range from

75.48 to 96.14% and 79.16 to 97.69%, respectively (Table 2). Wet gas (C₂₊) contents vary from 0.85 to 8.44% for the gas fields and from 2.10 to 19.55% for the gas hydrate samples (Table 2). Dryness coefficients (C₁/C₁₋₅ by volume) were in the range of 0.91–0.95 (Table 2). The δ¹³C₁, δ¹³C₂, and δ¹³C₃ values of all gas fields and W08 range from –59.5 to 35.97‰, –28.40 to 22.40‰, and –27.80‰ to –20.20‰, respectively. The δ¹³C values of the CO₂ samples vary from –20.70‰ to –2.70‰ in the gas fields (Table 2).

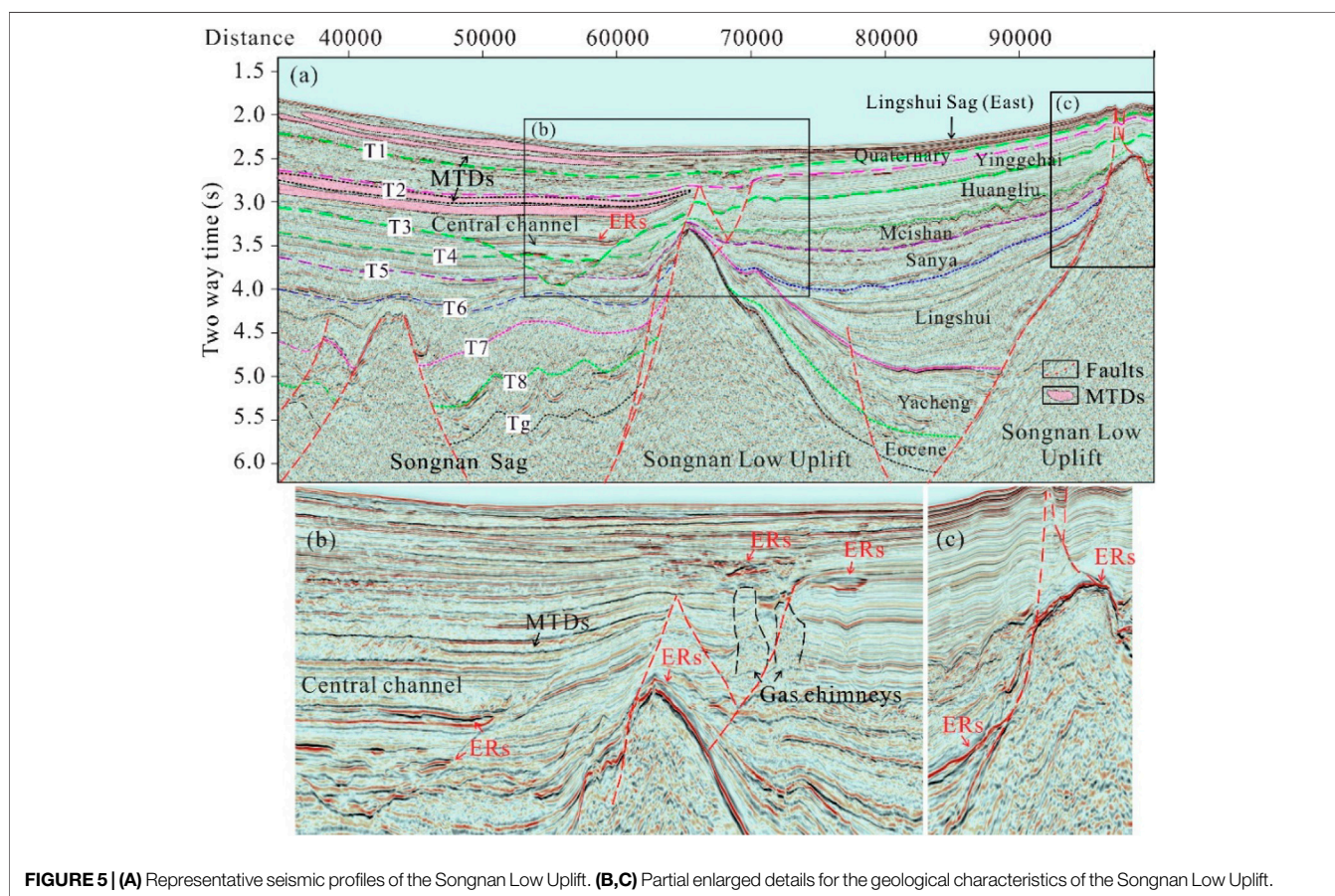
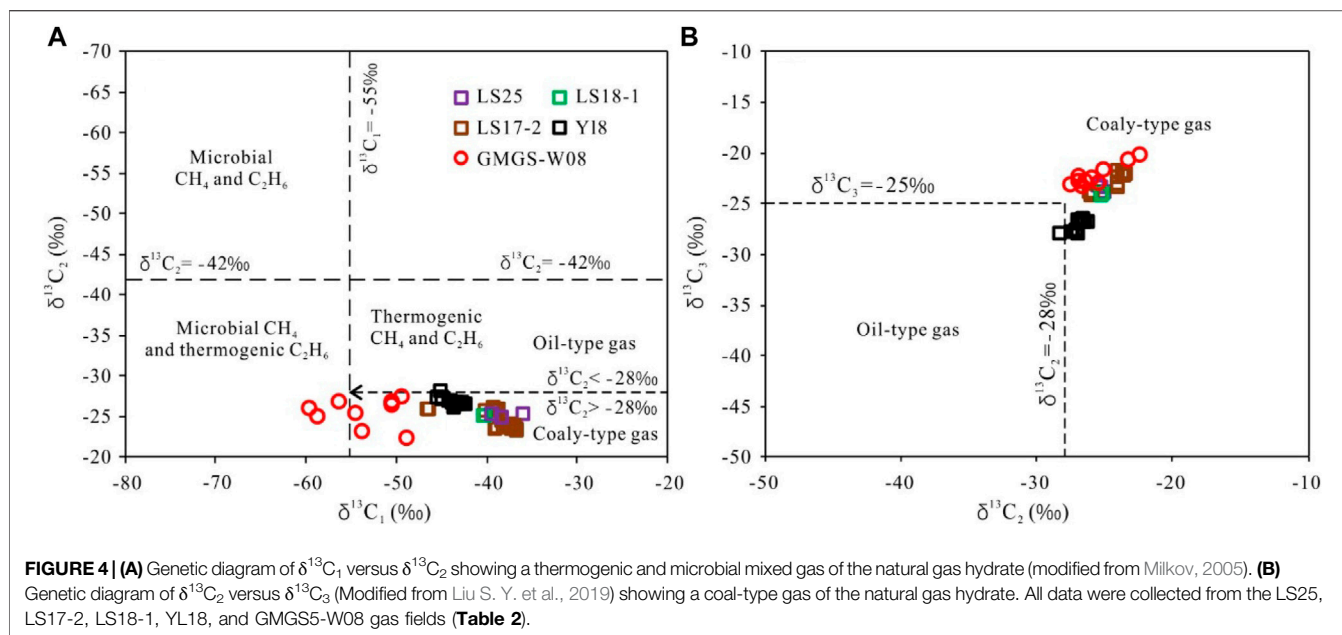
Previous studies suggested that δ¹³C₁ and δ¹³C₂ threshold values to distinguish thermogenic and microbial origins of CH₄ and C₂H₆ are –55‰ and –42‰, respectively, (Milkov, 2005). Thermogenic gas can be subdivided into coal-type and oil-type gas by δ¹³C₂ and δ¹³C₃ threshold values of –28‰ and –25‰, respectively (Xu and Shen, 1996; Huang et al., 2016; Liu Q. et al., 2019; Lai et al., 2021). A plot of the δ¹³C₁ values versus the δ¹³C₂ values of the analyzed gas samples shows that methane (CH₄) in both the gas hydrates and gas fields was composed of thermo-

TABLE 2 | Gas composition and isotopic composition of the LS25, LS17-2, LS18-1, YL8-1, and YL8-3 large gas fields and hydrate-related gas at site GMGS-W08 in the QDNB. (Data were collected from Liang et al., 2015; Zhang et al., 2019a; Zhang et al., 2019b; Li et al., 2020; Lai et al., 2021; Yang et al., 2021; Zhu et al., 2021).

Well	Depth (m)	Formation	Gas compositions (%)				C1/(C1-C5)	$\delta^{13}\text{C}$ (‰)			
			C1	C2+	CO2	N2		C1	C2	C3	CO2
LS25 gas field											
LS25-1	3,760.8	Huangliu	87.31	7.83	3.08	1.79	0.92	-39.37	-25.39	-23.30	-8.97
	3,920.0~890.0		85.17	7.77	6.08	0.97	0.92	-38.30	-25.15	-23.71	-3.68
LS25-2	4,094.0		81.38	8.07	8.89	1.33	0.91	-35.97	-25.57	-23.13	-4.53
LS17-2 gas field											
LS17-1	3,306.0	Huangliu	90.04	5.94	0.9	2.97	0.94	-36.93	-23.63	-22.09	-16.42
	3,366.4		91.05	5.75	0.68	2.37	0.94	-37.30	-23.62	-21.89	-16.39
LS17-2	3,331.3		91.55	5.93	0.07	2.17	0.94	-37.55	-24.09	-22.96	-18.03
LS22-1-1	3,339.0		91.16	7.98	0.31	0.55	0.92	-39.20	-26.20	-23.80	/
	3,352.5		91.37	7.75	0.32	0.57	0.93	-38.80	-26.00	-23.70	/
	3,391.0		91.53	7.59	0.32	0.55	0.93	-39.20	-26.00	-24.10	/
LS17-2-1	3,306.0		92.51	6.38	0.45	0.68	0.94	-36.81	-23.51	-21.97	/
	3,324.0		93.25	5.93	0.21	0.62	0.94	-36.78	-23.62	-22.17	/
	3,366.4		92.69	6.21	0.46	0.63	0.94	-37.25	-23.77	-21.87	/
	3,468.5		92.56	6.31	0.52	0.61	0.94	-36.83	-24.09	-21.58	/
LS1728N1	3,305.2		/	/	/	/	/	-40.15	-25.94	/	/
LS1728N2	3,406.5		/	/	/	/	/	-38.89	-25.95	/	/
LS1727N3	3,477.0		/	/	/	/	/	-46.46	-26.12	/	/
LS1724N4	3,251.0		/	/	/	/	/	-39.07	-25.37	/	/
LS1724N6	3,355.0		/	/	/	/	/	-39.15	-23.61	/	/
LS1724N7	3,445.0		/	/	/	/	/	-38.36	-24.57	/	/
L17-B	3,228.5		91.68	5.90	0.70	1.66	0.94	-38.20	-23.80	-21.80	-20.70
L17-A	3,321.0~3,351.0		93.00	5.97	0.62	0.26	0.94	-37.30	-24.10	-22.20	-9.20
L17-G	3,477.0		83.38	8.44	0.30	5.87	0.91	-46.50	-26.10	-24.00	-15.70
LS18-1 gas field											
LS18-1	2,819.9~2,846.7	Yinggehai	93.17	6.27	0.05	0.51	0.94	-40.46	-25.17	-23.82	/
LS18-A	2,819.9~2,846.7		92.89	6.24	0.04	0.64	0.94	-40.20	-25.30	-24.00	/
YL8-1 gas field											
YL8-1	/	Yacheng	/	/	/	/	0.97	-45.20	-28.40	-27.80	/
	/	Pre-tertiary	/	/	/	/	0.97	-44.90	-27.40	-27.70	/
YL8-1	/	Sanya	/	/	/	/	0.98	-45.50	-27.50	-27.60	/
	/	Yacheng	/	/	/	/	0.98	-44.00	-27.10	-27.80	/
	/	Pre-tertiary	/	/	/	/	0.99	-42.70	-26.90	/	/
YL8-1-A	2,956.7	Mesozoic	94.50	2.97	0.60	1.80	0.98	-45.00	-27.50	-27.60	-16.00
YL8-1-A	2,988.2		94.60	3.05	0.50	1.70	0.98	-44.20	-27.20	-27.40	-17.20
YL8-1-B	3,070.0		84.02	0.85	14.08	1.03	0.99	-43.80	-26.90	/	-8.90
YL8-1-B	3,354.0		75.48	0.90	19.07	4.55	0.99	-42.40	-26.80	/	-8.90
YL8-3 gas field											
YL8-3	/	Pre-tertiary	/	/	/	/	0.97	-43.20	-26.80	-26.50	/
YL8-3	/	Yacheng	/	/	/	/	0.97	-43.30	-26.70	-26.50	/
	/	Pre-tertiary	/	/	/	/	0.97	-43.40	-26.70	-26.40	/
YL8-3-A	2,828.8~2,936.0	Mesozoic	95.67	3.22	0.83	0.19	0.97	-42.70	-26.60	-26.60	-2.70
YL8-3-B	2,894.0	Yacheng	95.68	3.08	0.37	0.85	0.97	-43.30	-27.00	-26.80	-16.40
YL8-3-B	2,905.0	Yacheng	90.36	2.94	0.32	6.39	0.97	-43.70	-26.30	-26.70	-17.60
YL8-3-B	2,911.0	Yacheng	96.14	3.19	0.22	0.44	0.97	-43.30	-27.00	-26.50	-17.60
GMGS5-W08 gas hydrate drilling site											
GH-1	8.0	Quaternary	97.69	2.10	/	/	/	-59.50	-26.00	-22.40	/
PCS-1	32.9		94.94	4.81	/	/	/	-54.40	-25.50	-22.90	/
GH-2	62.9		81.21	17.46	/	/	/	-56.30	-26.90	-22.70	/
PCS-2	79.0		95.75	4.08	/	/	/	-58.60	-25.10	-21.60	/
PCS-3	80.9		95.73	4.04	/	/	/	-48.80	-22.40	-20.20	/
PCS-4	112.3		96.46	3.32	/	/	/	-53.80	-23.30	-20.70	/
PCS-5	145.7		83.49	15.54	/	/	/	-49.30	-27.50	-23.00	/
GH-3	148.4		79.16	19.55	/	/	/	-50.40	-26.50	-22.80	/
PCS-6	158.0		84.17	14.89	/	/	/	-50.40	-26.90	-22.20	/
PCS-7	187.1		92.82	6.63	/	/	/	-50.40	-26.70	-23.20	/

microbial methane (CH_4) and thermogenic methane (CH_4). Ethanes (C_2H_6) were derived solely from coal-type thermogenic gas with $\delta^{13}\text{C}_2$ values $> -28\text{‰}$ (Figure 4A).

A notable phenomenon is that the $\delta^{13}\text{C}_1$ values decreased from -35.97‰ to -59.5‰ along gas migration pathways (from LS25 to W08 or from the Sag Center to the Low Uplift),



indicating lighter $\delta^{13}C_1$ values due to fraction effects of secondary migration and increased contents of biogenic gas. The C_2+ hydrocarbon gas in the hydrate was mainly

derived from the deeply buried coal-type source rocks, and methane (CH_4) often has a mixed thermogenic and microbial origin.

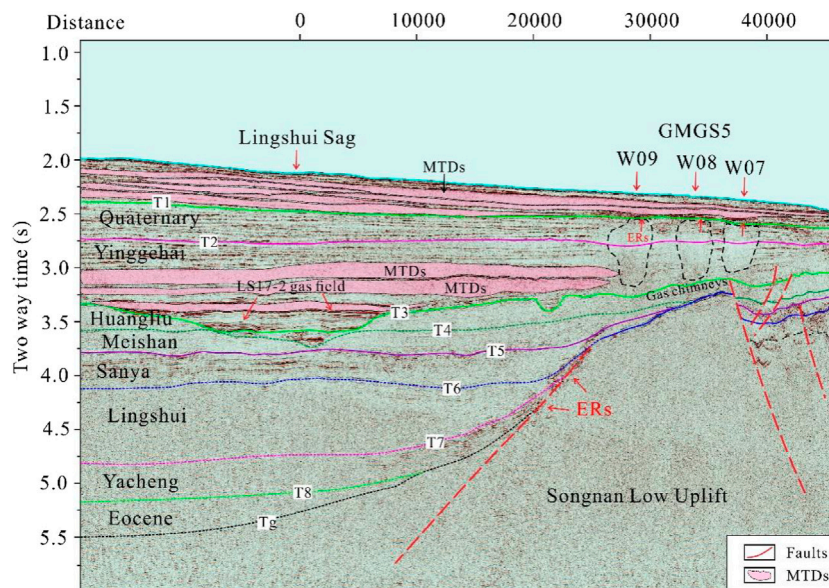


FIGURE 6 | Seismic reflection features of the bottom simulating reflector (BSR), diapirs, gas chimneys, and faults in the QDNB, showing the accumulation process of the hydrate-related gas at the site GMGS5-W08.

Migration Pathways

Natural gas hydrate accumulation, which is similar to the conventional oil and gas reservoirs, is often associated with faults, gas chimneys, and diapirism. Faults that fail to reach the gas hydrate stability zone (GHSZ) directly are not efficient pathways for hydrate accumulation that some large-scale faults, however, are often connected with gas chimneys to form efficient fluid migration pathway systems. Normal faults are identified in the study area, which extend from the source rocks to the Quaternary strata or connected with gas chimneys at shallower burial depths (Figure 5A), a characteristic indicating intense fluid migration from deep areas to the seafloor or shallow traps through the fault-chimney pathways. In parallel, enhanced reflections (ERs) were widely developed on the top of or at the flanks of the gas chimneys, faults, and central channel (Figures 5B,C), indicating significant fluid flow in the study area (Cartwright et al., 2007; Horozal et al., 2009; Petersen et al., 2010; Karstens & Berndt, 2015; Kang et al., 2016).

Gas chimneys were developed mainly in the Low Uplift, exhibiting vertical columnar or finger shapes (Figure 5B and Figure 6). The GMGS5 W07, W08, and W09 gas hydrate sites are located directly on the top of three large gas chimneys (Figure 6). Diameters of the gas chimneys vary from 3 to 5 km, and the top of the chimneys terminates at the T1 interface, ~150 m from the seafloor (Figure 6). Gas chimneys are characterized by mushroom-shaped acoustic blanking zones, with weak internal push-down reflections being interpreted (Figure 6). The high-amplitude reflections at the edge or within the gas chimneys were identified as high-velocity gas hydrate in the soft sediments (Figure 6). Normal faults were interpreted within the gas chimneys, with invisible faults and/or fractures beyond seismic

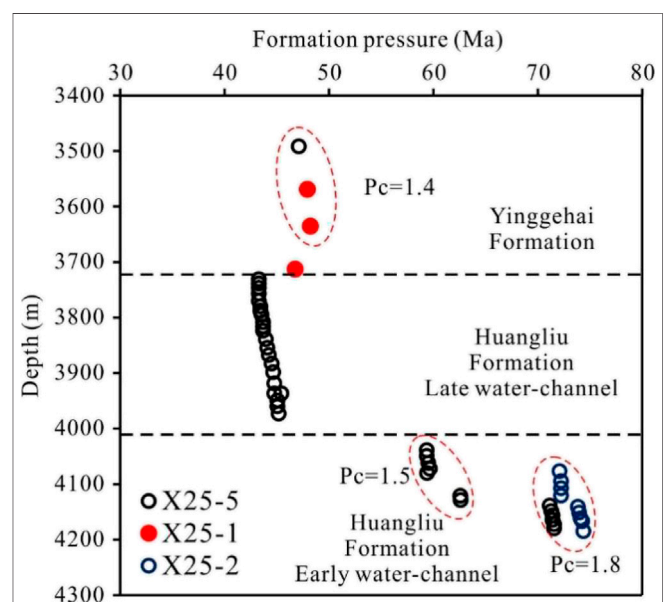


FIGURE 7 | Pressure distribution of LS25 gas fields in the Lingshui Sag (Li et al., 2021).

resolution being widely developed in the interior of the gas chimneys. With widely distributed enhanced reflections (ERs) on the top of or at the flanks of the gas chimneys (Figure 6), fluid charging should occur constantly in the study area.

Overpressures

Pressure and temperature, especially overpressure, are important driving forces for sub-surface fluid flow, and understanding their

TABLE 3 | Homogenization temperatures (Ths) of coexisting aqueous inclusions and hydrocarbon charging time (HCT) of the large gas fields in the Lingshui Sag.

Location	Formation	Inclusion type	Th (°C)	HCT (Ma)	Reference
Well W-6 (LS17)	Huangliu	Hydrocarbon-bearing	100–240 peak value 160–180	0.4–0.6	Xu et al. (2014)
LS17 gas field	Huangliu	Aqueous	Stage I: 78–90.2	2–0	He, (2020)
LS25 gas field			Stage II: 99.7–101.2	2–0	
X17 gas field (LS17)	Huangliu	Hydrocarbon-bearing	Stage I: 87.2	0.3	Gan et al. (2019)
			Stage II: 110–120	0.2	
			Stage III: 140–160	0.0	

origins and evolution is the key aspect to understand oil and gas migration and accumulation mechanisms.

In the LS25 gas field of the QDNB, two separate overpressure systems were identified (Figure 7, Gan et al., 2019). The lower overpressure system is mainly formed by hydrocarbon generation, with a maximum pressure coefficient (Pc) > 1.8, which extends up to the bottom of the Huangliu Formation. The upper overpressure system is in the second member of the Yinggehai Formation, which was subject to rapid subsidence and disequilibrium compaction of the shallow marine mudstones, with a pressure coefficient (Pc) of c. 1.4. Gas accumulation in the Huangliu Formation (from 1.8 Ma to the present) is relatively later than that in the second member of the Yinggehai overpressured interval, indicating that gas accumulation in the late Huangliu channel system occurred between the formation of the two high-pressure systems since 1.8 Ma, a timing with large-scale hydrocarbon generation and migration. Two thick gas layers in the early and late phases of channel depositions have pressure coefficients of 1.5 and 1.0, respectively. Sandstone intervals deposited early in the channel have a pressure coefficient (Pc) up to 1.8, a characteristic indicating poor gas preservation conditions of upper units of the channel due to the development of intense fractures.

Gas generated source rocks were accumulated in the distinct reservoirs of the channel system by overpressure and buoyancy, with continuous upward migration into the second member of the Yinggehai Formation being hindered by the existence of the upper overpressure system. However, the fluid can be migrated laterally along the porous sandstones in the channels which were proved by the discovery of the LS18 gas field, east of the Central Canyon.

Hydrocarbon-Charging Stages

Fluid inclusion can be applied to confirm phases of oil and gas accumulation, which record important information on fluid properties, trapping temperatures, and pressures under *in situ* conditions. Hydrocarbon-bearing aqueous inclusions and aqueous inclusions were widely developed in the Huangliu Formation in the LS25 and LS17-2 gas fields in the Lingshui Sag (Xu et al., 2014; Gan et al., 2018; He, 2020). Homogenization temperatures (Ths) of the hydrocarbon-bearing aqueous inclusions are >120°C, ranging from 130 to 160°C. The Ths of the aqueous inclusions range from 78 to 90.2°C and from 99.7 to 101.2°C in wells LS17-2-7 and LS25-3-1, respectively, which is significantly lower than that of the hydrocarbon-bearing aqueous inclusions (He, 2020).

At least three hydrocarbon charging stages were identified in the study area according to the Ths of the hydrocarbon-bearing aqueous inclusions in the Huangliu Formation of the LS17 gas field, corresponding to Ths of 87.2°C, 110–120°C, and 140–160°C, respectively (Gan et al., 2019; Table 3). Timing for hydrocarbon charging is estimated to be c. 0.3 Ma at a temperature of 87.2°C. Some of the Ths of the hydrocarbon-bearing aqueous inclusions are relatively higher than the current strata temperature (approximately 100°C), indicating the influence of deep thermal fluids/gas in the Central Canyon gas fields in the Lingshui Sag, which were driven by the deep high-pressure/temperature fluid systems.

In addition, hydrocarbon-bearing aqueous inclusions and the coexisting aqueous inclusions were commonly developed in the target formation, indicating multi-stages of fluid migration in the QDNB. The Ths of the coexisting aqueous inclusions range from 78 to 90.2°C and from 99.7 to 101.2°C in wells LS17 and LS25 in the Lingshui Sag, matching a trapping time of 2–0 Ma (Table 3).

The previous study indicates four stages of hydrocarbon and fluid migration stages in the QDNB, with charging times from 17.5 to 13 Ma (Stage I), 10 to 5.5 Ma (Stage II), 4 to 2 Ma (Stage III), and 2 to 0 Ma (Stage VI), respectively (Figure 8) (Liu and Chen, 2011; Huang et al., 2012; Xu et al., 2014; Su et al., 2016a, 2016b; Xu et al., 2017; Gan et al., 2018; Zhong et al., 2019; He, 2020).

Natural Gas Hydrate Accumulation Mechanism

Based on the geochemical analysis, paleotemperature/pressure and hydrocarbon charging analyses, and the structural characteristics of the QDNB, preliminary accumulation models for natural gas hydrates were proposed in the Songnan Low Uplift (Figure 9).

Prior to the accumulation processes forming gas hydrates, favorable hydrocarbon generation conditions, efficient migration pathways, and sufficient driving forces are key aspects to form gas hydrates. TOC contents and Rock-Eval results indicate good hydrocarbon generation potential of the Yacheng and Lingshui source rock formations, which are highly matured or over-matured. Effective hydrocarbon migration systems in the study area mainly comprise faults, laterally distributed extended channel sandstones, and gas chimneys. Faults that extend from the source rock intervals up to the Quaternary strata or gas chimneys provide efficient hydrocarbon migration pathways. In the LS25 gas field, late deposition in the channel of the Huangliu Formation has a Pc value of 1.0, and the early deposited intervals in the channel have Pc values of 1.5–1.8, which are significantly higher. Some of the Pc

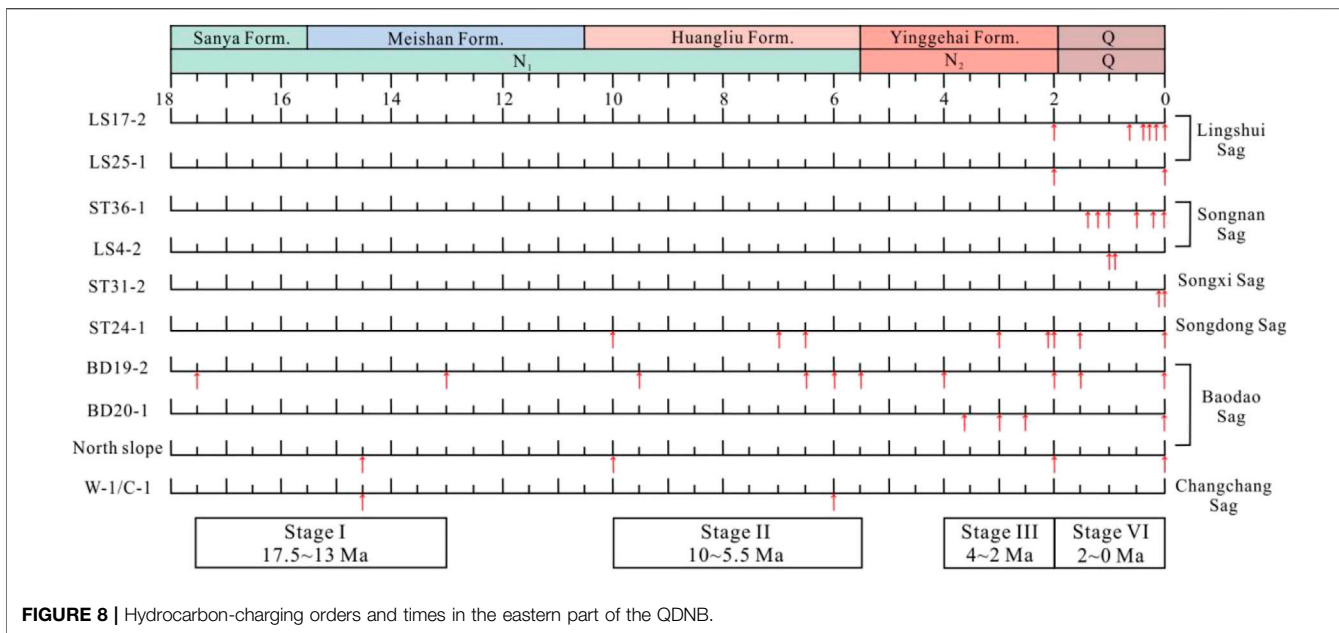


FIGURE 8 | Hydrocarbon-charging orders and times in the eastern part of the QDNB.

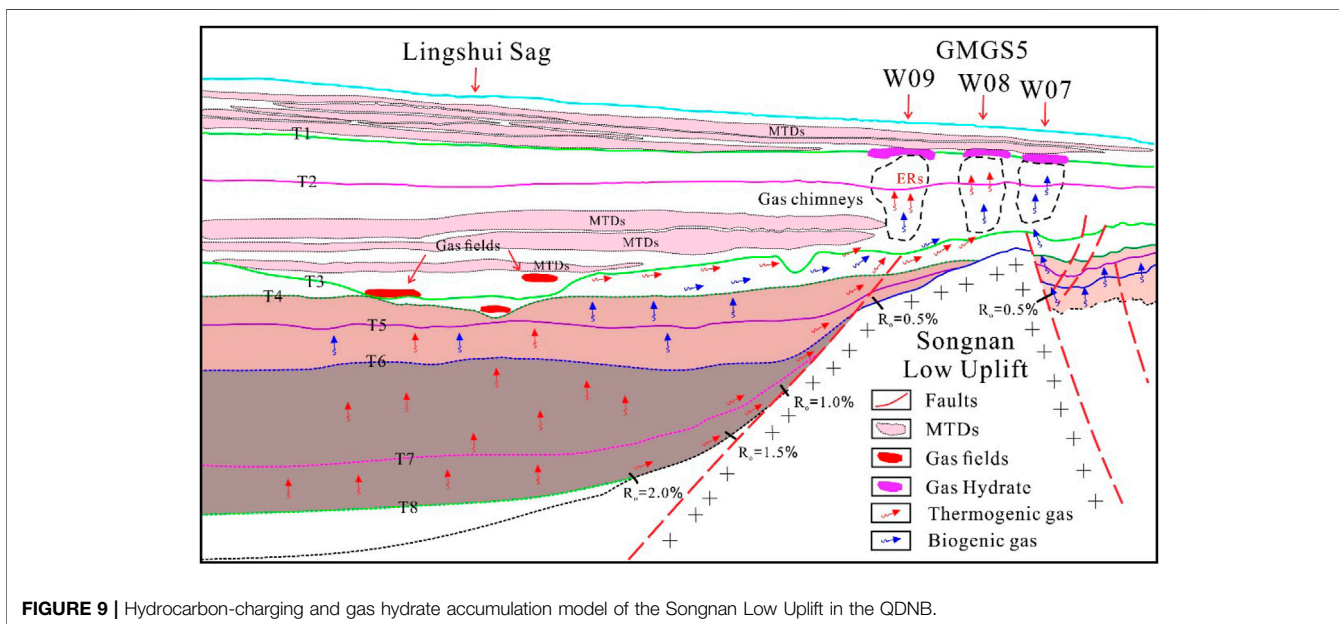


FIGURE 9 | Hydrocarbon-charging and gas hydrate accumulation model of the Songnan Low Uplift in the QDNB.

values in the Yacheng Formation can even reach 2.1 (Zhang et al., 2016), indicating that strong overpressure at depth can provide sufficient impetus for hydrocarbon migration.

With our analysis, high-overmatured thermogenic gas was postulated to be derived from mudstone or coal-bearing strata of the Oligocene Yacheng and Lingshui formations. Gases in the Lingshui Sag could migrate upward through faults. Meanwhile, natural gas was also migrated through laterally distributed sandstone due to the sealing effect of the MTDs (Figure 9). Furthermore, migration of gas was mixed with shallow biogenic gas, thus forming the gas hydrate, such as the cases of the W09 and W08 gas hydrates (Figure 9). Biogenic gas derived from immature or low mature source

rocks of the shallow Sanya and Meishan formations can also migrate through faults to form gas hydrates in the study area, such as the W07 gas hydrates (Figure 9). A mixture of biogenic gas in the study area can also be the result of diffusion through interbedded microcracks and pore networks in the shallower strata.

CONCLUSION

Detailed geochemical analysis, paleotemperature and paleopressure analyses, seismic interpretation, and hydrocarbon charging characterization were conducted to

investigate the controlling factors of natural gas hydrate accumulation. Our research reaches the following conclusions.

- (1) The Yacheng and Lingshui formations with high-overmatured source rocks are effective to generate thermogenic gas, and the Meishan and Sanya formations with immature to low matured source rocks can provide abundant biogenic gas.
- (2) Large-displacement faults, laterally distributed sandstones, and overpressure are the main driving force and migration pathways for the formation of gas hydrates at shallow burial depths.
- (3) Four stages of fluid migration occurred in the QDNB, with stage IV (2~0 Ma) hydrocarbon migration as the main stage of gas hydrate formation.
- (4) The natural gas hydrate accumulation model was subscribed into two types: large-scale fault migration and lateral migration of thermogenic gases to form the hydrate in shallow sediments.

DATA AVAILABILITY STATEMENT

The original contributions presented in the study are included in the article/Supplementary Material, further inquiries can be directed to the corresponding author.

REFERENCES

- Cartwright, J., Huuse, M., and Aplin, A. (2007). Seal Bypass Systems. *Bulletin* 91, 1141–1166. doi:10.1306/04090705181
- Deng, W., Liang, J., Zhang, W., Kuang, Z., and He, Y. (2021). Typical Characteristics of Fracture-Filling Hydrate-Charged Reservoirs Caused by Heterogeneous Fluid Flow in the Qiongdongnan Basin, Northern South China Sea. *Mar. Pet. Geology*. 124, 104810. doi:10.1016/j.marpetgeo.2020.104810
- Fang, Y., Wei, J., Lu, H., Liang, J., Lu, J. a., Fu, J., et al. (2019). Chemical and Structural Characteristics of Gas Hydrates from the Haima Cold Seeps in the Qiongdongnan Basin of the South China Sea. *J. Asian Earth Sci.* 182, 103924. doi:10.1016/j.jseaes.2019.103924
- Gan, J., Wu, D., Zhang, Y., Liu, S., Guo, M., Li, X., et al. (2019). Distribution Pattern of Present-Day Formation Temperature in the Qiongdongnan Basin: Implications for Hydrocarbon Generation and Preservation. *Acta Metallurgica Sinica* 25 (6), 952–960. doi:10.16108/j.issn.1006-7493.2019053
- Gan, J., Zhang, Y. Z., and Liang, G. (2018). On Accumulation Process and Dynamic Mechanism of Natural Gas in the Deep-Water Area of Central Canyon, Qiongdongnan Basin. *Acta Geol. Sin.* 92 (11), 2359–2362. doi:10.3969/j.issn.0001-5717.2018.11.011
- Hao, F., Zou, H., Gong, Z., Yang, S., and Zeng, Z. (2007). Hierarchies of Overpressure Retardation of Organic Matter Maturation: Case Studies from Petroleum Basins in China. *Bulletin* 91 (10), 1467–1498. doi:10.1306/05210705161
- He, C., Gan, J., Liang, G., Li, X., Wang, X., Li, T., et al. (2021). Characteristics of the Organic Carbon Isotope of Oligocene Source Rocks in deepwater Area of the Qiongdongnan Basin and its Main Controlling Factors. *Geochemical* 50 (2), 175–184. PhD thesis.
- He, C. M. (2020). *Geochemistry and Hydrocarbon Generation of Source Rocks and Origins of Natural Gases in the deepwater Area of the Qiongdongnan Basin*. [PhD thesis]. Guangzhou: Guangzhou institute of Geochemistry, Chinese Academy of Science.
- He, T., Li, W., Lu, S., Pan, W., Ying, J., Zhu, P., et al. (2022). Mechanism and Geological Significance of Anomalous Negative $\delta^{13}\text{C}$ kerogen in the Lower Cambrian, NW Tarim Basin, China. *J. Pet. Sci. Eng.* 208, 109384. doi:10.1016/j.petro.2021.109384
- He, T., Lu, S., Li, W., Tan, Z., and Zhang, X. (2018). Effect of Salinity on Source Rock Formation and its Control on the Oil Content in Shales in the Hetaoyuan Formation from the Biyang Depression, Nanxiang Basin, Central China. *Energy Fuels* 32, 6698–6707. doi:10.1021/acs.energyfuels.8b01075
- Horozal, S., Lee, G. H., Yi, B. Y., Yoo, D. G., Park, K. P., Lee, H. Y., et al. (2009). Seismic Indicators of Gas Hydrate and Associated Gas in the Ulleung Basin, East Sea (Japan Sea) and Implications of Heat Flows Derived from Depths of the Bottom-Simulating Reflector. *Mar. Geology*. 258, 126–138. doi:10.1016/j.margeo.2008.12.004
- Hu, B., Wang, L., Yan, W., Liu, S., Cai, D., Zhang, G., et al. (2013). The Tectonic Evolution of the Qiongdongnan Basin in the Northern Margin of the South China Sea. *J. Asian Earth Sci.* 77, 163–182. doi:10.1016/j.jseaes.2013.08.022
- Huang, B., Li, L., and Huang, H. (2012). Origin and Accumulation Mechanism of Shallow Gases in the North Baodao Slope, Qiongdongnan Basin, South China Sea. *Pet. Exploration Develop.* 39, 567–573. doi:10.1016/s1876-3804(12)60077-9
- Huang, B., Tian, H., Li, X., Wang, Z., and Xiao, X. (2016). Geochemistry, Origin and Accumulation of Natural Gases in the deepwater Area of the Qiongdongnan Basin, South China Sea. *Mar. Pet. Geology*. 72, 254–267. doi:10.1016/j.marpetgeo.2016.02.007
- Huang, B., Xiao, X., and Li, X. (2003). Geochemistry and Origins of Natural Gases in the Yinggehai and Qiongdongnan Basins, Offshore South China Sea. *Org. Geochem.* 34, 1009–1025. doi:10.1016/s0146-6380(03)00036-6
- Huang, H. T., Huang, B. J., Huang, Y. W., Li, X., and Tian, H. (2017). Condensate Origin and Hydrocarbon Accumulation Mechanism of the Deepwater Giant Gas Field in Western South China Sea: a Case Study of Lingshui 17-2 Gas Field in Qiongdongnan Basin, South China Sea. *Pet. Exploration Develop.* 44 (3), 380–388. doi:10.1016/s1876-3804(17)30047-2
- Kang, N.-k., Yoo, D.-g., Yi, B.-y., and Park, S.-c. (2016). Distribution and Origin of Seismic Chimneys Associated with Gas Hydrate Using 2D Multi-Channel Seismic Reflection and Well Log Data in the Ulleung Basin, East Sea. *Quat. Int.* 392, 99–111. doi:10.1016/j.quaint.2015.08.002
- Karstens, J., and Berndt, C. (2015). Seismic Chimneys in the Southern Viking Graben - Implications for Palaeo Fluid Migration and Overpressure Evolution. *Earth Planet. Sci. Lett.* 412, 88–100. doi:10.1016/j.epsl.2014.12.017

AUTHOR CONTRIBUTIONS

YW and RJ wrote the whole manuscript and provided all figures. NZ, XC, and LH gathered and prepared data. CR provided all tables. KZ, LJ, and LH contributed to the discussion and outline. ZB, CJ, ZX, and LL improved the grammar of writing.

FUNDING

This article was granted by the Key Special Project for Introduced Talents Team of Southern Marine Science and Engineering Guangdong Laboratory (Guangzhou) (Grant No. GML2019ZD0102), the State Key Laboratory of Organic Geochemistry, GIGCAS (Grant No. SKLOG 2020**), and the Guangdong Basic and Applied Basic Research Foundation (No. 2020A1515110405).

ACKNOWLEDGMENTS

The authors are grateful to all participants of the fifth China National Gas Hydrate Drilling Expedition (GMGS5) during the preparation of this manuscript.

- Lai, H., Fang, Y., Kuang, Z., Ren, J., Liang, J., Lu, J. a., et al. (2021). Geochemistry, Origin and Accumulation of Natural Gas Hydrates in the Qiongdongnan Basin, South China Sea: Implications from Site GMGS5-W08. *Mar. Pet. Geology*. 123, 104774. doi:10.1016/j.marpetgeo.2020.104774
- Li, J. S., Li, X. Q., Wang, Y., Wang, G., Xu, X. D., and Liu, H. Y. (2021). Geochemical Characteristics and Hydrocarbon Generation Potential Evaluation of Source Rocks in Deep-Water Area of Qiongdongnan Basin. *J. Mining Sci. Technol.* 6 (2), 166–175. doi:10.19606/j.cnki.jmst.2021.02.004
- Li, X., Gan, J., Yang, X., Laing, G., and Wang, Z. L. (2020). Characterization of Natural Gas Migration in the Ancient Buried hill, East Deep-Water Area of Qiongdongnan Basin. *Nat. Gas Geosci.* 31 (7), 970–979. doi:10.11764/j.issn.1672-1926.2020.02.007
- Li, X. S., Zhang, Y. C., Yang, X. B., Xu, X. F., Zhang, J. X., and Man, X. (2017). New Understanding and Progress of Natural Gas Exploration in Yinggehai-Qiongdongnan Basin. *China Offshore Oil and Gas* 29 (6), 5–15. doi:10.11935/j.issn.1673-1506.2017.06.001
- Liang, G., Gang, J., and Li, X. (2015). Genetic Types and Origin of Natural Gas in Lingshui Sag, Qiongdongnan Basin. *China Offshore Oil Gas* 27, 47–53. (In Chinese with English abstract). doi:10.11935/j.issn.1673-1506.2015.04.006
- Liang, J., Zhang, W., Lu, J. a., Wei, J., and Kuang, Z. (2019). Geological Occurrence and Accumulation Mechanism of Natural Gas Hydrates in the Eastern Qiongdongnan basin of the South China Sea: Insights from Site GMGS5-W9-2018. *Mar. Geology*. 418, 106042. doi:10.1016/j.margeo.2019.106042
- Liu, Q., Wu, X., Wang, X., Jin, Z., Zhu, D., Meng, Q., et al. (2019). Carbon and Hydrogen Isotopes of Methane, Ethane, and Propane: a Review of Genetic Identification of Natural Gas. *Earth-Science Rev.* 190, 247–272. doi:10.1016/j.earscirev.2018.11.017
- Liu, S. Y., Chen, H. Y., Li, D. Y., Sun, W. Y., and Li, C. Y. (2019). Sedimentary Characteristics and Source Rock Development Model of the Oligocene Lingshui Formation in Lingshui Sag, Qiongdongnan Basin. *Mar. Origin Pet. Geology*. 24 (01), 63–70. doi:10.3969/j.issn.1672-9854.2019.01.008
- Liu, Z., and Chen, H. (2011). Hydrocarbon Charging Orders and Times in the Eastern Area of Qiongdongnan Basin. *Geoscience* 25 (2), 279–288. doi:10.1007/s12182-011-0123-3
- Milkov, A. V. (2005). Molecular and Stable Isotope Compositions of Natural Gas Hydrates: a Revised Global Dataset and Basic Interpretations in the Context of Geological Settings. *Org. Geochem.* 36, 681–702. doi:10.1016/j.orggeochem.2005.01.010
- Petersen, G. J., Bünz, S., Hustoft, S., Mienert, J., and Klaeschen, D. (2010). High-resolution P-Cable 3D Seismic Imaging of Gas Chimney Structures in Gas Hydrated Sediments of an Arctic Sediment Drift. *Mar. Pet. Geology*. 27 (9), 1981–1994. doi:10.1016/j.marpetgeo.2010.06.006
- Shi, H. S., Yang, J. H., Zhang, Y. Z., Gan, J., and Yang, J. H. (2019). Geological Understanding Innovation and Major Breakthrough to Natural Gas Exploration in Deep Water in Qiongdongnan Basin. *China Pet. Exploration* 24 (6), 691–698. doi:10.3969/j.issn.1672-7703.2019.06.001
- Su, A., Chen, H., Chen, X., Liu, H., Liu, Y., and Lei, M. Z. (2018). New Insight into Origin, Accumulation and Escape of Natural Gas in the Songdong and Baodao Regions in the Eastern Qiongdongnan basin, South China Sea. *J. Nat. Gas Sci. Eng.* 52, 467–483. doi:10.1016/j.jngse.2018.01.026
- Su, A., Chen, H., He, C., Lei, M., and Liu, Y. (2017). Complex Accumulation and Leakage of YC21-1 Gas Bearing Structure in Yanan Sag, Qiongdongnan Basin, South China Sea. *Mar. Pet. Geology*. 88, 798–813. doi:10.1016/j.marpetgeo.2017.09.020
- Su, A., Chen, H. H., He, C., Zhai, P. Q., Liu, Y. H., and Lei, M. Z. (2016b). The Characteristic of Fluid Activities and Diagenetic Responses of the Pressure Discharging Zone in Yacheng Area, Qiongdongnan Basin, South China Sea. *Acta Petrolei sinica* 37 (10), 1216–1230. doi:10.7623/syxb201610002
- Su, A., Chen, H., Yang, W., Feng, Y. X., Zhao, J. X., and Lei, M. Z. (2021). Hydrocarbon Gas Leakage from High-Pressure System in the Yanan Sag, Qiongdongnan Basin, South China Sea. *Geol. J.* 56, 5094–5108. doi:10.1002/gj.4225
- Su, A., Du, J. M., Chen, H. H., Yu, Y., and Lei, M. Z. (2016a). Diagenetic Fluid Type and Activity History of Controlling the Development of Abnormal Pore Zone: Taking the north Margin of Baodao Sag, Qiongdongnan Basin as an Example. *Nat. Gas Geosci.* 27 (10), 1837–1847. doi:10.11764/j.issn.1672-1926.2016.10.1837
- Wang, P., Li, S., Suo, Y., Guo, L., Santosh, M., Li, X. Y., et al. (2021). Structural and Kinematic Analysis of Cenozoic Rift Basins in South China Sea: A Synthesis. *Earth-Science Rev.* 216 (2), 103522. doi:10.1016/j.earscirev.2021.103522
- Wang, Y., Li, X. Q., Liang, W. L., Sun, K. X., Zhang, M., Xu, X. D., et al. (2018). Characteristics of Saturated Hydrocarbon Biomarkers and the Biogenetic Composition of Source Rocks in the Qiongdongnan Basin. *J. Mining Sci. Technol.* 3 (3), 209–218. doi:10.19606/j.cnki.jmst.2018.03.001
- Wang, Z., Sun, Z., Zhang, Y., Guo, M., Zhu, J., Huang, B., et al. (2016). Distribution and Hydrocarbon Accumulation Mechanism of the Giant deepwater central canyon Gas Field in Qiongdongnan basin, Northern South China Sea. *China Pet. Exploration* 21 (4), 1–12. doi:10.3969/j.issn.1672-7703.2016.04.006
- Wei, J., Liang, J., Lu, J., Zhang, W., and He, Y. (2019). Characteristics and Dynamics of Gas Hydrate Systems in the Northwestern South China Sea - Results of the Fifth Gas Hydrate Drilling Expedition. *Mar. Pet. Geology*. 110, 287–298. doi:10.1016/j.marpetgeo.2019.07.028
- Xie, Y., Zhang, G., Sun, Z., Zeng, Q., Zhao, Z., and Guo, S. (2019). Reservoir Forming Conditions and Key Exploration Technologies of Lingshui 17-2 Giant Gas Field in deepwater Area of Qiongdongnan Basin. *Pet. Res.* 4, 1–18. doi:10.1016/j.ptlrs.2019.01.004
- Xu, H. Z., Zhang, Y. Z., Lin, C. M., Pei, J. X., and Liu, Y. Z. (2014). Characteristics and Key Controlling Factors of Natural Gas Accumulation in the central Submarine canyon, Qiongdongnan Basin. *Acta Geol. Sinica* 88 (9), 1741–1751. doi:10.3969/j.issn.0001-5717.2014.09.010
- Xu, X. D., Zhang, Y. Z., Xiong, X. F., Gan, J., and Liang, G. (2017). Genesis, Accumulation and Distribution of CO₂ in the Yinggehai-Qiongdongnan Basin, North South China Sea. *Mar. Geology. Front.* 33 (7), 45–54. doi:10.16028/j.1009-2722.2017.07.005
- Xu, Y., and Shen, P. (1996). A Study of Natural Gas Origins in China. *AAPG Bull.* 80, 1604–1614. doi:10.1306/64eda0c8-1724-11d7-8645000102c1865d
- Yang, X. B., Zhou, J., Yang, J. H., He, X. H., Wu, H., Gan, J., et al. (2021). Natural Gas Source and Accumulation Model of Mesozoic Buried hill in the Eastern Deep Water Area of Qiongdongnan Basin. *Acta Petrolei Sinica* 42 (3), 283–292. doi:10.7623/syxb202103002
- Yao, Z., Wang, Z. F., Zuo, Q. M., Sun, Z. P., Dang, Y. Y., Mao, X. L., et al. (2015). Critical Factors for the Formation of Large-Scale deepwater Gas Field in Central Canyon System of Southeast Hainan Basin and its Exploration Potential. *Acta Petrolei Sinica* 36 (11), 1358–1366. doi:10.7623/syxb201511005
- Ye, J., Wei, J., Liang, J., Lu, J., Lu, H., and Zhang, W. (2019). Complex Gas Hydrate System in a Gas Chimney, South China Sea. *Mar. Pet. Geology*. 104, 29–39. doi:10.1016/j.marpetgeo.2019.03.023
- Zhang, G. C., Zeng, Q. B., Su, L., Yang, H. Z., Chen, Y., Yang, D. S., et al. (2016). Accumulation Mechanism of LS 17-2 Deep Water Giant Gas Field in Qiongdongnan Basin. *Acta Petrolei Sinica* 37 (S1), 34–46. doi:10.7623/syxb2016S1004
- Zhang, G., Zhang, Y., Shen, H., and He, Y. (2014). An Analysis of Natural Gas Exploration Potential in the Qiongdongnan Basin by Use of the Theory of “Joint Control of Source Rocks and Geothermal Heat”. *Nat. Gas Industry B* 1, 41–50. doi:10.1016/j.ngib.2014.10.005
- Zhang, W., Liang, J. Q., Lu, J. A., Meng, M. M., He, Y. L., Deng, W., et al. (2020). Characteristics and Controlling Mechanism of Typical Leakage Gas Hydrate Reservoir Forming System in the Qiongdongnan Basin, Northern South China Sea. *Nat. Gas Industry* 40 (8), 90–99. doi:10.3787/j.issn.1000-0976.2020.08.007
- Zhang, W., Liang, J. Q., Su, P. B., Wei, J. G., Sha, Z. B., Lin, L., et al. (2018). Migrating Pathways of Hydrocarbons and Their Controlling Effects Associated with High Saturation Gas Hydrate in Shenhu Area, Northern South China Sea. *Geology. China* 45 (1), 1–14. doi:10.12029/gc20180101
- Zhang, Y. Z., Gan, J., Xu, X. D., Liang, G., and Li, X. (2019c). The Source and Natural Gas Lateral Migration Accumulation Model of Y8-1 Gas Bearing Structure, East Deep Water in the Qiongdongnan Basin. *Earth Sci.* 44 (8), 2609–2618. doi:10.3799/dqkx.2019.159
- Zhang, Y. Z., Li, X. S., Xu, X. D., Gan, J., Yang, X. B., Liang, G., et al. (2019b). Genesis, Origin, and Accumulation Process of the Natural Gas of L25 Gas Field in the Western deepwater Area, Qiongdongnan Basin. *Mar. Origin Pet. Geology*. 24 (3), 73–82. doi:10.3969/j.issn.1672-9854.2019.03.009
- Zhang, Y. Z., Xu, X. D., Gan, J., Yang, X. B., Zhu, J. T., Yang, J. H., et al. (2019a). Formation Condition and Accumulation of Pliocene Strata-Trapped Gas Field L18 in the deepwater Area of the Qiongdongnan Basin. *Haiyang Xuebao* 41 (3), 121–133. doi:10.3969/j.issn.0253-4193.2019.03.012
- Zhong, J., Yang, X., Zhu, P., Xu, S., Deng, X., Tuo, L., et al. (2019). Porosity Evolution Differences of the Lingshui Formation Reservoir between Baodao

- and Changchang Sag, Qiongdongnan Basin. *Earth Sci.* 44 (8), 2665–2676. doi:10.3969/j.issn.0253-4193.2019.03.012
- Zhu, W. L., Huang, B. J., Mi, L., Wilkins, R. W. T., Fu, N., and Xiao, X. M. (2009). Geochemistry, Origin, and Deep-Water Exploration Potential of Natural Gases in the Pearl River Mouth and Qiongdongnan Basins, South China Sea. *AAPG Bull.* 93, 741–761. doi:10.1306/02170908099
- Zhu, W., Shi, H., Huang, B., Zhong, K., and Huang, Y. (2021). Geology and Geochemistry of Large Gas fields in the deepwater Areas, continental Margin Basins of Northern South China Sea. *Mar. Pet. Geology.* 126, 104901. doi:10.1016/j.marpetgeo.2021.104901
- Zhu, Y., Sun, L., Hao, F., and Tuo, L. (2018). Geochemical Composition and Origin of Tertiary Oils in the Yinggehai and Qiongdongnan Basins, Offshore South China Sea. *Mar. Pet. Geology.* 96, 139–153. doi:10.1016/j.marpetgeo.2018.05.029

Conflict of Interest: Author LL was employed by the company Beijing International Engineering Consulting Co., Ltd.

The remaining authors declare that the research was conducted in the absence of any commercial or financial relationships that could be construed as a potential conflict of interest.

Publisher's Note: All claims expressed in this article are solely those of the authors and do not necessarily represent those of their affiliated organizations, or those of the publisher, the editors, and the reviewers. Any product that may be evaluated in this article, or claim that may be made by its manufacturer, is not guaranteed or endorsed by the publisher.

Copyright © 2022 Wei, Zenggui, Jinfeng, Jinqiang, Hong, Zijie, Chenlu, Hongfei, Rui, Bin, Jing, Xi and Lei. This is an open-access article distributed under the terms of the Creative Commons Attribution License (CC BY). The use, distribution or reproduction in other forums is permitted, provided the original author(s) and the copyright owner(s) are credited and that the original publication in this journal is cited, in accordance with accepted academic practice. No use, distribution or reproduction is permitted which does not comply with these terms.